ISTITUTO NAZIONALE DI FISICA NUCLEARE

Sezione di Trieste

INFN/TC-97/33
28 Ottobre 1997

E. Falk, V. Hedberg, I. Gouz, G. Della Ricca:

ALGORITHMS FOR REDUCTION OF COHERENT NOISE IN THE SILICON SHOWER MAXIMUM DETECTOR OF STIC

SIS–Pubblicazioni
dei Laboratori Nazionali di Frascati

INFN – Istituto Nazionale di Fisica Nucleare
Sezione di Trieste

INFN/TC–97/33
28 Ottobre 1997

Algorithms for Reduction of Coherent Noise in the Silicon Shower Maximum Detector of STIC

E. Falk, V. Hedberg
Department of Physics, University of Lund, Lund, Sweden
I. Gouz
Institute for High Energy Physics, Protvino, Russia
G. Della Ricca
Dipartimento di Fisica, Università di Trieste and INFN, Trieste, Italy

Abstract

Three algorithms to reduce coherent noise in the silicon shower maximum detector of the DELPHI luminosity monitor STIC are described. The simplest method is fast enough to be used on-line in the readout chain. This would allow one to select the channels to be read out and hence a great reduction of the volume of data. The results of tests of the efficiency and the accuracy of this algorithm are presented, as well as a comparison with the other two methods that also have been proposed for coherent-noise correction.

1 Introduction

The luminosity monitor STIC in DELPHI consists of two lead-scintillator calorimeters of shashlik type, read out by wavelength-shifting fibers and placed on either side of the interaction point [1]-[7]. Each calorimeter has been equipped with two planes of silicon-strip shower maximum detectors, providing a tracking facility, the main purpose of which is to reject off-energy electron background [3]-[7]. Reduction of coherent noise in data read out from these silicon detectors is an essential step in the data processing in order to ensure accurate reconstruction of the energy and the position of the shower. In addition, it is important to have a tool to reduce the amount of information to read out from the silicon detectors, which consist of approximately 4000 channels. A fast algorithm to reduce coherent noise on-line would permit localization of showers and thereafter readout of only a small selection of silicon-strip channels in the vicinity of these showers.

We present a fast and simple, yet accurate, method to reduce coherent noise from the STIC silicon detectors, a method which meets both of the above requirements. It needs no information from any other detector and could be implemented at an early stage of the readout chain, *i.e.,* in the Sirocco IV Fastbus modules, where the signals from the silicon-strip detectors are digitized, and which are equipped with digital signal processors (DSPs) [3]-[7]. A description of the algorithm itself is given, together with the results of an evaluation thereof and a comparison with two other proposed methods to reduce coherent noise.

2 Geometry and Readout of Silicon Detectors

The two calorimeters of STIC are made up of lead-scintillator sandwich layers, which are divided into 10 rings and 16 sectors. They are usually referred to as arm A and arm C, according to the DELPHI convention of calling the side of incoming electrons side A and that of positrons side C. The silicon detectors consist of planes of circular strips replacing one lead-scintillator layer at a depth of 4.0 radiation lengths and another at 7.4 radiation lengths in each of the two arms of STIC, thus giving a total of four silicon planes. Each silicon plane is divided into 16 sectors that follow the sector geometry of the calorimeter; each sector contains 60 strips and thus makes up a 22.5° segment of 60 concentric circles [3]-[7]. Two such sectors in a plane are connected to one Microplex MX4 amplifier chip with an input capacity of 128 channels. The strips are connected to the MX4 by Kapton[1] cables (see Figure 1), which are matched to the input of the MX4 by a hybrid fan-in card. The Kapton cables have a capacity of either 12 or 20 channels. The 24 innermost strips of each sector are read out by two 12-channel Kapton cables and the other 36 strips by two 20-channel Kapton cables. The outermost cable reads out only 16 strips and thus leaves four empty channels connected to the MX4 [3]-[7].

[1]Registered trademark of DuPont

3 Background and Motivation

The method for coherent-noise reduction that is proposed here processes raw silicon-strip data event by event in only two steps in order to allow the possibility of on-line implementation, which would be critical in both processing time and memory requirements. The first step subtracts pedestals, and the second step calculates and subtracts coherent noise.

3.1 Pedestals

Pedestals can be calculated on-line with good accuracy using only a small subsample of events and without use of any external trigger or calorimeter information. Due to sampling conditions (*i.e.*, a positive baseline for the digitization of strip signals) which are altered at the beginning of each physics run, the pedestals must be calculated for each new run. However, one need not use STIC triggers to do this; one may use any DELPHI trigger in order to establish new pedestals as quickly as possible at the beginning of the run. If, amongst these triggers, there are STIC showers for which one does not wish to lose information from the silicon detectors, one can simply read out all silicon-strip channels for these events and process them off-line.

3.2 Coherent Noise

The origin of the coherent noise in the silicon-strip detectors of STIC is not entirely understood. One possible source is electromagnetic pick-up from external devices. Another possibility is noise being generated internally by the front-end electronics (preamplifiers etc.) due to a parasitic electrical coupling between inputs and outputs. It is clear, however, that there is correlation in the noise between channels of the same Kapton cable. There is also noise correlation between channels of adjacent Kapton cables, *i.e.*, cables which belong to the same fan-in card and which emerge from the detector along the same path and are placed on top of one another. Other patterns of coherence are also present, but they are less important. It is necessary to make use of the correlation between channels that are located some distance apart in order to find coherent pulse-height shifts over strip areas larger than a shower, which is typically wider than 20 strips; otherwise, one would not be able to determine the amplitude of the coherent noise at the location of the shower.

Our method makes use of the correlation between Kapton cables. The same pattern of correlation applies to most, but not all, fan-in cards. Therefore, look-up tables are used to store the correlations. There is one such table for each fan-in card, and the table contains 8×8 entries, one for each pair of Kapton cables of the fan-in card in question. For simplicity, each entry is either 1 or 0, depending upon whether or not there is strong correlation with a slope near unity. At present, correlations other than those with a slope near 1 are not included, although such exist and some of them can be relatively strong. The tables have been established manually after a study of plots of the correlation of the average pulse height for each pair of Kapton cables within a fan-in card and over a large number of events. Examples of such correlation plots are shown in Figure 2. For reasons not fully understood, the correlations vary slightly from year to year, so the correlation tables must be updated occasionally and checked a few times per year.

4 Algorithm

As mentioned in the previous section, the method proposed here processes data in two steps; first, pedestals are subtracted, and then coherent noise is calculated and subtracted. The algorithm consists of two separate parts; one performed at the beginning of each new physics run in order to establish pedestal values for each silicon strip, and one for the rest of the run which carries out pedestal and coherent-noise correction.

4.1 Calculation of Pedestals On-line

The first 100 DELPHI triggers at the beginning of a physics run are used to calculate pedestals in two steps: *i)* The signal of each of the first 50 events is added for each individual strip, and then one calculates the mean, p_i', and RMS, r_i', for each strip i. *ii)* The operation is repeated for the following 50 events, but for each strip one now includes only those events for which the signal passes the cut $a_i \leq p_i' + 2r_i'$, where p_i' and r_i' are those obtained from the first 50 events. This selection is made in order to minimize the influence of showers. The mean, p_i, and RMS, r_i, obtained after the second calculation are those that will be used as pedestal values for the remainder of the run.

Optionally, this procedure can be repeated on every set of 100 events and the pedestal values used only for the following 100 events instead of for the remainder of the run. This would take care of any sudden jumps in the pedestals during a run. (This phenomenon occurred a few times during the datataking of 1995 and has not been explained.)

4.2 Calculation of Pedestals Off-line

The calculation of the coherent-noise correction is independent of the way in which the pedestal values are calculated and may well be used together with pedestals calculated according to a different method. In order to evaluate the accuracy of the on-line pedestal algorithm, an off-line method was also used.

The off-line method calculates pedestal values using most, but not all, of the events of a physics run. Reconstructed calorimeter clusters are used to discard events with more than one shower per arm. For events with zero calorimeter clusters in one of the arms, all the strips of that arm are used. For events with one cluster, only the strips of the sector located opposite the one through which the shower passed are used; see Figure 3 for an illustration of the selection procedure. This minimizes the influence of showers without restricting the event selection to "empty" events only. The pedestal mean and RMS for each strip are defined to be the mean and RMS of the pulse heights of the selected events.

4.3 Correction for Pedestals and Coherent Noise

After the first 100 triggers of a run, each event is treated as follows: The pedestal mean value obtained at the beginning of the run (or, optionally, at the latest pedestal calculation) is subtracted from the raw data of each strip, a_i, *i.e.*,

$$a_i' = a_i - p_i.$$

Thereafter, one calculates, for each Kapton cable k, the average pulse height $< a >_k$ of all the Kapton cables that are correlated to k (according to the look-up table discussed above). In this calculation only those strips are included which fulfil

$$a_i' \leq n r_i,$$

where n is a constant which is typically 2–3. The purpose of this cut is once again to exclude showers. The value obtained is the estimate of the coherent noise for the group of strips belonging to the Kapton cable in question. This is subtracted from each channel of the Kapton cable, so that one obtains a corrected pulse height for each strip, a_i'':

$$a_i'' = a_i' - < a >_k .$$

After having applied the above correction to all Kapton cables, one reads out only those strips for which the pulse height passes a suitably chosen threshold.

5 Evaluation

In order to obtain a good understanding of the performance of the coherent-noise correction method, the coherent-noise correction itself and the calculation of pedestals were evaluated separately.

The evaluation described below, as well as the development of the algorithm itself and the comparison with other algorithms, were performed on data from LEP run 61020 taken at 45 GeV in July 1995. The silicon detectors were read out only for Bhabha-triggered events at that time. Not all of the recorded events were used, but a subsample containing approximately 14000 events from the beginning of the run were used as test data.

5.1 Evaluation of Coherent-Noise Correction

The signal amplitudes obtained after coherent-noise correction were compared in two ways to those obtained before correction (but after pedestal subtraction). First, the pulse heights were plotted for the strips of each fan-in card before and after correction. Two examples, one for each arm, are shown in Figures 4 and 5. As expected, the data that have been corrected for coherent noise show a much narrower distribution around zero ADC counts than the data that are only pedestal-corrected; the coherent-noise correction clearly reduces the spread around zero. Moreover, after coherent-noise correction, hardly any events populate the region below the band where the bulk of the events are concentrated, which indicates that the tables of correlations between Kapton cables have been established correctly.

Second, the pulse-height distributions of all the strips of each fan-in card were studied for two different cases: In the first case, events were selected when a shower passed through one of the two sectors read out by the fan-in card in question. In the second case, the selection was made for events where the shower went through one of the sectors opposite those of the fan-in card. This selection was made to minimize the influence of showers, since the data sample used contained only Bhabha-triggered events. The selection procedure is illustrated in Figure 3. As in the calculation of off-line pedestals, the determination of the location of showers was based upon reconstructed clusters in the calorimeter arms. The distributions were compared to those obtained before coherent-noise correction but after pedestal subtraction. Figure 6 shows one example of each case from each arm. The coherent-noise correction was found to reduce greatly the width of the pulse-height distribution for all fan-in cards. The peak of the distribution after correction is at zero ADC counts. In the presence of showers, the distribution has a long tail towards higher values, as one would expect.

It is important to ensure that the calculation of the average pulse height used to correct the pedestal-subtracted signals in the vicinity of a shower is not biased by the shower itself. The correction applied to a signal by the coherent-noise correction algorithm was studied for two different cases, which are similar to those described above. The calorimeter was used to locate the sector through which a shower had passed. In one case, the strip with the maximum amplitude in this sector was selected, whereas in the other case, the corresponding strip in the sector opposite the one through which the shower had passed was selected; again, see Figure 3. The correction applied to these two strips is the difference between their pulse heights before and after coherent-noise correction. The average correction for each Kapton cable over all the events in the data sample was plotted for each of these two cases; a sample from each arm is shown in Figures 7(a) and (b). If there is no bias of the correction close to a shower, the average corrections must be the same with and without showers. There is indeed good, albeit not perfect, agreement between the two cases. However, in comparison with the width of the correction distributions, this difference is small and the bias negligible; see Figure 8 for an example of correction distributions in the presence and in the absence of showers.

The RMS cut in the calculation of $< a >_k$ was determined after a study of the way in which different cuts affect the pulse-height distribution after coherent-noise correction. If the cut is set too low, some of those strips which are not part of the shower but which populate the upper end of the pedestal distribution are excluded from the calculation of $< a >_k$. This results in an under-correction of the signal, and the pulse-height distributions far away from a shower will no longer be centered around zero. Too high a cut, on the other hand, includes strips which are indeed part of the shower in the calculation of $< a >_k$, and hence it yields an over-correction of the pulse height in the vicinity of the shower. Results of a very soft cut at $10r_i$ are shown in Figures 7 (c) and (d) as an illustration of the effects of over-correction when parts of showers are included in the coherent-noise calculation. The biased pulse-height correction in the presence of showers is clearly visible in Figure 7. Figure 9 compares pulse-height distributions of all the strips of a fan-in card in the absence and in the presence of showers for cuts at $10r_i$ and $2r_i$. The higher cut produces very good pedestal distributions in the absence of showers, whereas the lower cut results in a slight "overpopulation" of the tail on the positive side. This is due to fluctuations of the pedestal above the $2r_i$ cut. When several strips in the calculation of the coherent noise fluctuate above the cut, the calculated value becomes an underestimate of the noise, resulting in a tail in the pedestal distribution. In the presence of showers, however, a cut at $10r_i$ leads to many strips with a signal from the shower entering the noise calculation. The consequence is an overestimated noise value and an over-corrected pedestal with a tail towards negative values. In this case, the cut at $2r_i$ behaves better. In the end, a cut at $3r_i$ was chosen.

An estimate of how many strips would remain to be read out after coherent-noise correction was obtained through a count of the number of strips with pulse heights $a_i > 3r_i$ after coherent-noise correction. For the bulk of events with one reconstructed cluster, *i.e.*, one shower, in the calorimeter arm, there remain less than 50 channels to read out on side A and less than 70 on side C. The corresponding numbers for the few events in the data sample with no shower in the calorimeter are 30 and 10 channels respectively. These distributions are shown in Figure 10. The fraction of events with one calorimeter cluster and no silicon strips to read out is 3%.

The coherent-noise correction method where a correction factor is calculated and applied in one step thus succeeds in reducing coherent noise without over-correcting the signal in the vicinity of a shower, and it permits a great reduction in the number of strips to be read out for each event.

5.2 Evaluation of On-Line Pedestal Algorithm

Pedestals calculated off-line according to the method described in Section 4.2 were used as reference pedestals to which those calculated on-line were compared. Results obtained after coherent-noise reduction, where the two different sets of pedestals had been used prior to noise correction, were also compared.

The number of events needed to calculate pedestals at the beginning of a run was determined after a study of the difference between pedestal mean values of the two methods as a function of the number of events. The mean values calculated without cuts fluctuate somewhat with the number of events used, due to the influence of showers. The second step, however, where a cut on the RMS (obtained in the first step) is applied, seems rather insensitive to these fluctuations. With 50 events used to calculate the first set of pedestals, the second set seem to be reasonably stable after less than 50 additional events. The choise was therefore made to use $50+50$ events at the beginning of each run to calculate pedestals. An example of the difference between the on-line and off-line pedestal mean and RMS values after the second iteration as a function of the number of events is shown in Figure 11.

The quality of the RMS values obtained using $50+50$ events was verified through a comparison of the distributions of the RMS values of the two pedestal methods. These distributions agree very well, as can be seen in Figure 12. 100 events is thus sufficient to obtain good RMS values.

In the previous subsection, the average pulse-height corrections calculated and applied by the coherent-noise reduction algorithm were discussed. These corrections were also studied when the reference pedestals had been used before coherent-noise correction. It was found that the two pedestal methods produce very similar results, as can be seen in Figure 13.

Finally, the optional method of recalculating the pedestals on each set of 100 events was compared to that of calculating them only once at the beginning of a new run. The average pulse-height corrections applied, as well as the pulse heights of all strips after coherent-noise correction, are very similar for the two methods.

These tests thus show that only 100 events are needed to calculated adequate pedestal mean and RMS values for the whole run with the proposed two-step scheme. This makes it possible to calculate pedestals on-line, which is necessary for on-line coherent-noise correction.

6 Comparison with Other Methods for Reduction of Coherent Noise

The tests described above were also performed on the other two methods for coherent-noise reduction, which were developed primarily for off-line use, and the results of the three algorithms were compared. For the sake of simplicity, we will refer to these two methods as methods B and C respectively and to the method described above as A.

6.1 Method B

The principle of method B is as follows: The coherent-noise correction is preceded by a conventional pedestal subtraction; pedestals which have been computed off-line at a previous stage are subtracted from the signal of each strip. Then the coherent noise is calculated and subtracted in four steps. First, the average pulse height of all strips is calculated. This value is subtracted from each strip. This procedure is carried out a second time, but now only strips which have a signal of less than 100 ADC counts are included. Then, individual fan-in cards are treated separately; the average signal of all strips of a fan-in card, without cuts, is calculated and subtracted from each of its strips. The last step treats groups of Kapton cables within each fan-in card: the four 12-channel Kapton cables reading out the 24 innermost strips of the two sectors of a fan-in card make up one group; the 20 following strips of each sector, read out by two 20-channel cables, make up a second group; the 16 last strips of the two sectors, also read out by two 20-channel cables, make up a third; and the four empty channels of these two cables make up a fourth group. The average pulse height of each group, where only strips which have a signal less than its RMS are included, is calculated. This is subtracted from all the strips of the group. The value that is then obtained for each strip is the coherent-noise corrected pulse height.

6.2 Method C

In method C the coherent-noise correction is done using individual noise-correlation coefficients for every strip. Only the noise correlations between strips of one sector are taken into account. To a good approximation, these coefficients are the components of the eigenvector corresponding to the largest eigenvalue of the noise covariance matrix for the strips of the sector. Since the largest eigenvalue in each sector is much larger than all of the others, the noise is clearly dominated by the coherent component, and this approximation is therefore valid. The correlation coefficients are calculated together with pedestals in a separate run prior to the data processing. The noise RMS with and without the coherent-noise correction and quality flags for the strips are determined in the same run.

During the data processing, the coherent-noise correction procedure is carried out after the conventional pedestal subtraction. The correction procedure operates on individual sectors and consists of subtraction from each signal a_i within the sector the value proportional to its noise correlation coefficient v_i :

$$a_i' = a_i - \kappa_s v_i \ , \quad \text{where}$$
$$\kappa_s = \frac{\sum_i a_i v_i}{\sum_i v_i^2}.$$

In the calculations of κ_s only those strips can be included which do not contain signals from showers. The calculations are therefore done iteratively, repeating the subtraction procedure three times. After each time the average RMS r_s for the sector is calculated,

$$r_s = \sqrt{\frac{1}{N}\sum a_i^2} \ ,$$

where N is the number of accepted strips, and those strips for which $a_i > 3r_s$ are then excluded from the calculation of κ_s in the next iteration.

6.3 Comparison

The signal amplitudes after coherent-noise correction by the three methods are shown in Figures 14 and 15. All three methods reduce the spread in the band around zero with respect to the situation previous to coherent-noise correction; see Figures 4 and 5. In general, methods A and C have very little occupancy below the band around zero ADC counts; in some cases it is smaller for method A, whereas in others it is smaller for method C. Method B, however, shows certain regions, which correspond to Kapton cables, where there is a relatively large occupancy below this band. This could be an indication of incorrectness in the assumption on correlation between some Kapton cables in this method.

Examples of the pulse-height distributions of all the strips of a fan-in card in the absence and in the presence of showers are shown on both linear and logarithmic scales in Figure 16. In the absence of showers, method C produces distinctly narrower distributions around zero ADC counts than the other two methods. In the presence of showers, the body of the distribution of method C is often asymmetric around zero, with a larger occupation of negative values. In certain cases it even extends below the pedestal distribution. This might indicate that the calculation of the correction by method C is somewhat influenced by the presence of showers.

A comparison of the pulse-height corrections applied by the three methods, studied in the same fashion as earlier, can be found in Figure 17. It shows that all three methods apply average corrections very near zero ADC counts in the absence of showers. A count of the number of strips remaining after a cut at $3r_i$ performed on methods B and C yields practically identical results to those of method A.

The three methods thus produce similar results, with the exception of method C which gives narrower pedestals than the other two in the absence of showers and perhaps over-corrects the pulse height somewhat in the presence of showers. Methods B and C are not directly applicable on-line, since they make use of data calculated off-line, such as pedestals, but they could be modified for on-line use, for instance by implementing the on-line pedestal algorithm proposed here. In the view of the complexity of the algorithms, however, method A should be better suited than the other two to meet on-line constraints.

7 Conclusions

The method for coherent-noise correction for the STIC silicon detectors described here is simple enough to be used on-line in order to reduce the amount of data to read out from these detectors. After pedestal subtraction, a coherent-noise term is defined to be the average pulse height of correlated Kapton cables, with a cut on the RMS of each strip in order to limit the influence of showers. This value is then subtracted from the pedestal-corrected signal. This procedure reduces coherent noise without over-correcting the pulse height of a shower. Tests show that pedestals can be calculated for each LEP run with good accuracy using about 100 events at the beginning of the run or, optionally, using sets of 100 events throughout the run. Comparisons with two other algorithms proposed for reduction of coherent noise show that the least complex method performs as well as the other two in terms of accuracy and should be well suited for on-line use.

8 Acknowledgements

The authors gladly acknowledge the many fruitful discussions and ideas contributed by T. Camporesi. We would also like to thank E. Migliore for shedding light on the readout of the silicon-strip detectors.

References

[1] S. J. Alvsvaag et al., *The Small Angle Tile Calorimeter project in DELPHI,* DELPHI 95-12 CAL 119, Contribution to the 4th International Conference on Advanced Technology and Particle Physics, Como, Italy, October 1994.

[2] S. J. Alvsvaag et al., *The DELPHI Small Angle Tile Calorimeter,* DELPHI 94-157 CAL 120, Contribution to the IEEE 1994 Nuclear Science Symposium and Medical Imaging Conference, Norfolk, USA, October 1994.

[3] S. J. Alvsvaag et al., *The new small angle calorimeter in DELPHI,* DELPHI 94-148 CAL 118, Contribution to the 5th International Conference on Calorimetry, Brookhaven, USA, September 1994.

[4] S. J. Alvsvaag et al., *The DELPHI Small Angle Tile Calorimeter,* DELPHI 95-14 CAL 123, Contribution to the Beijing Calorimetry Symposium, Beijing, China, October 1994.

[5] S. J. Alvsvaag et al., *The Silicon Shower Maximum Detector for the STIC,* DELPHI 94-126 CAL 117, Contribution to the 6th Pisa Meeting on Advanced Detectors, Elba, Italy, May 1994.

[6] S. J. Alvsvaag et al., *A silicon pad shower maximum detector for a "Shashlik" calorimeter,* DELPHI 94-158 CAL 121, Contribution to the IEEE 1994 Nuclear Science Symposium and Medical Imaging Conference, Norfolk, USA, October 1994.

[7] S. J. Alvsvaag et al., *A Silicon Pad Shower Maximum Detector for a Shashlik Calorimeter,* DELPHI 95-13 CAL 122, Contribution to the 4th International Conference on Advanced Technology and Particle Physics, Como, Italy, October 1994.

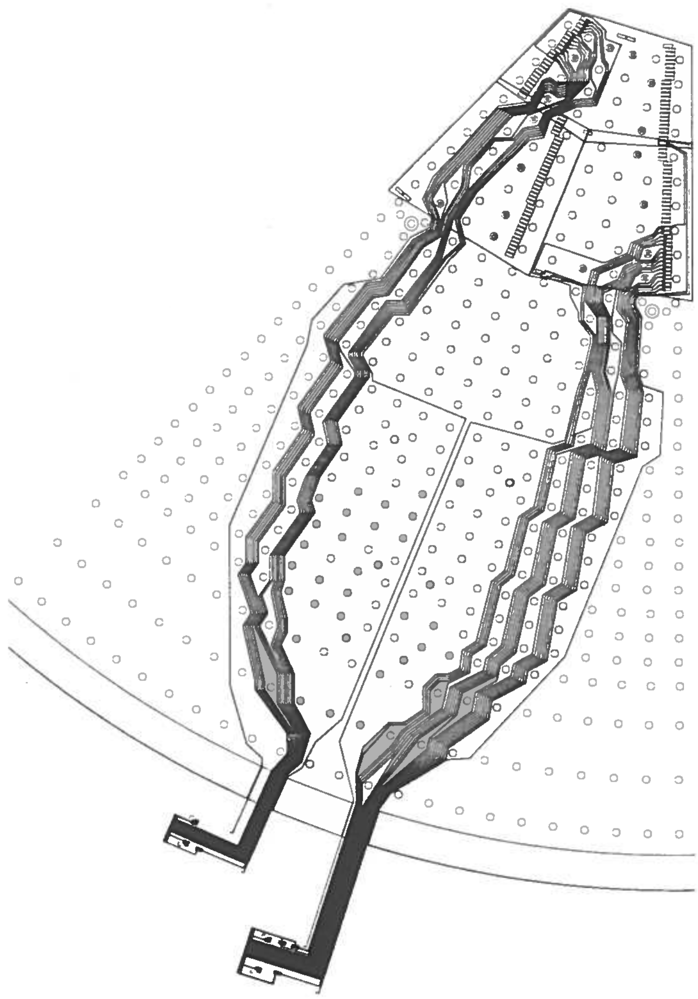

Figure 1: A 45° wedge (two 22.5° sectors) of the silicon shower maximum detector, with two of its eight Kapton cables shown. The strip structure within the sectors is not indicated. Note the many holes for the calorimeter fibers, which the signal wires have to avoid.

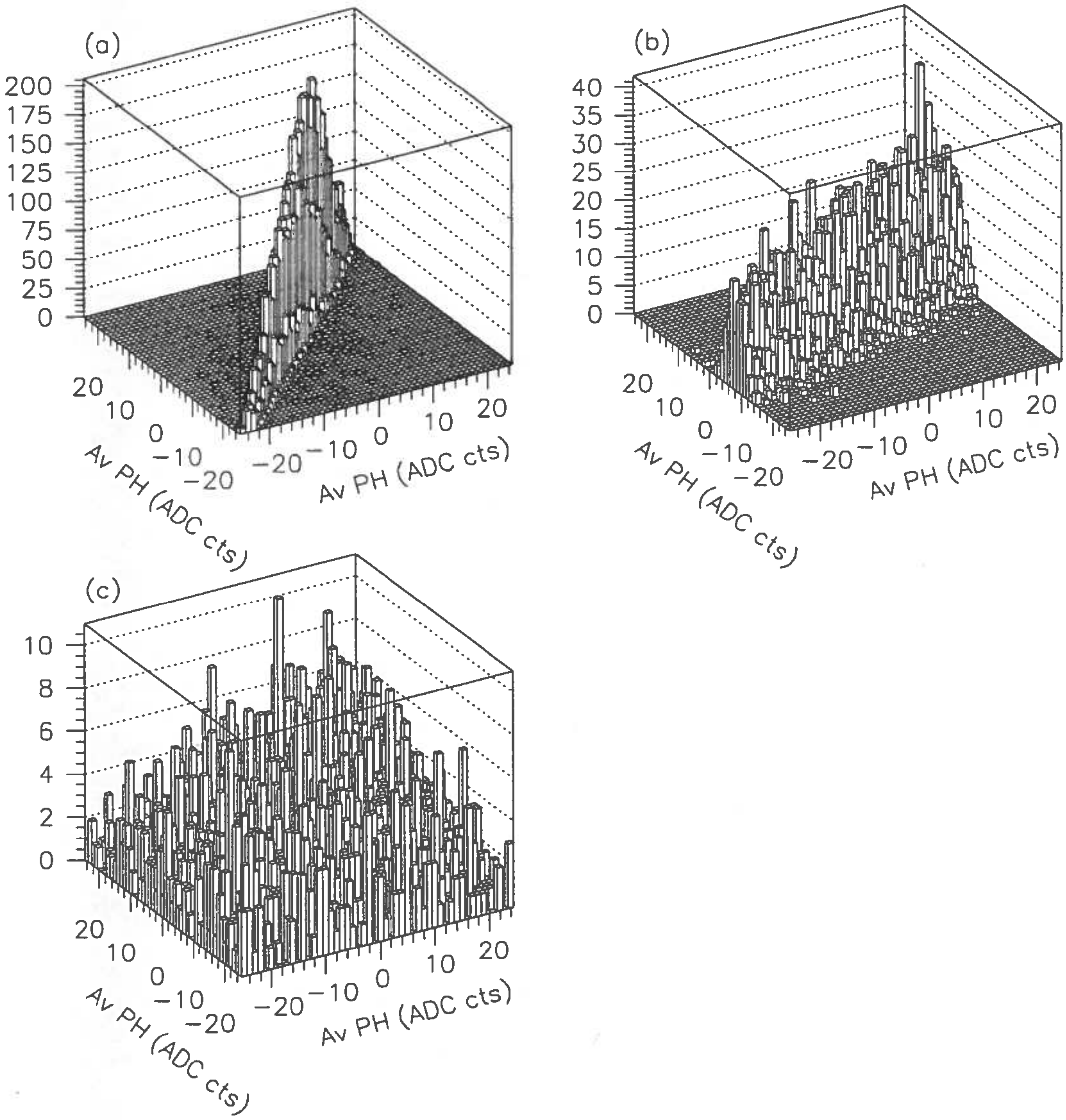

Figure 2: Examples of (a) "strong" correlation, (b) "weak" correlation, and (c) "no" correlation between the average pulse heights of pairs of Kapton cables.

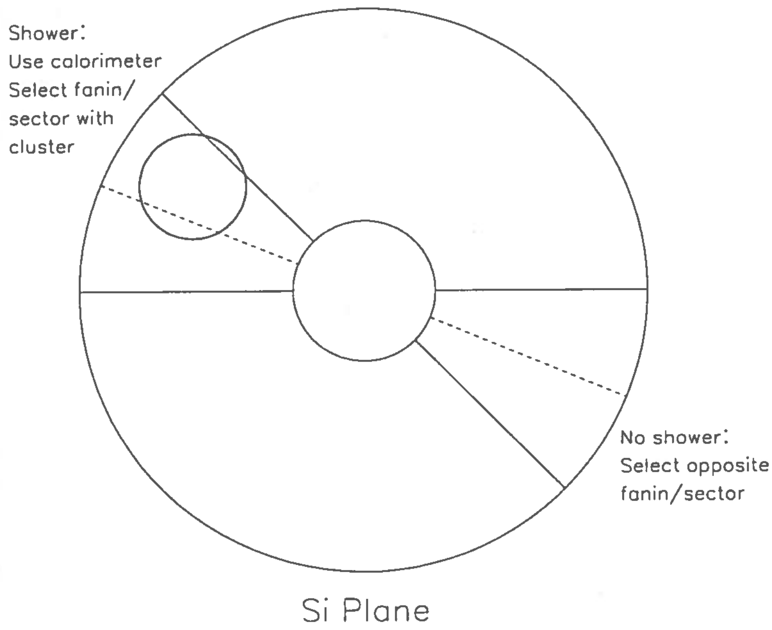

Figure 3: Selection of fan-ins/sectors, with and without showers.

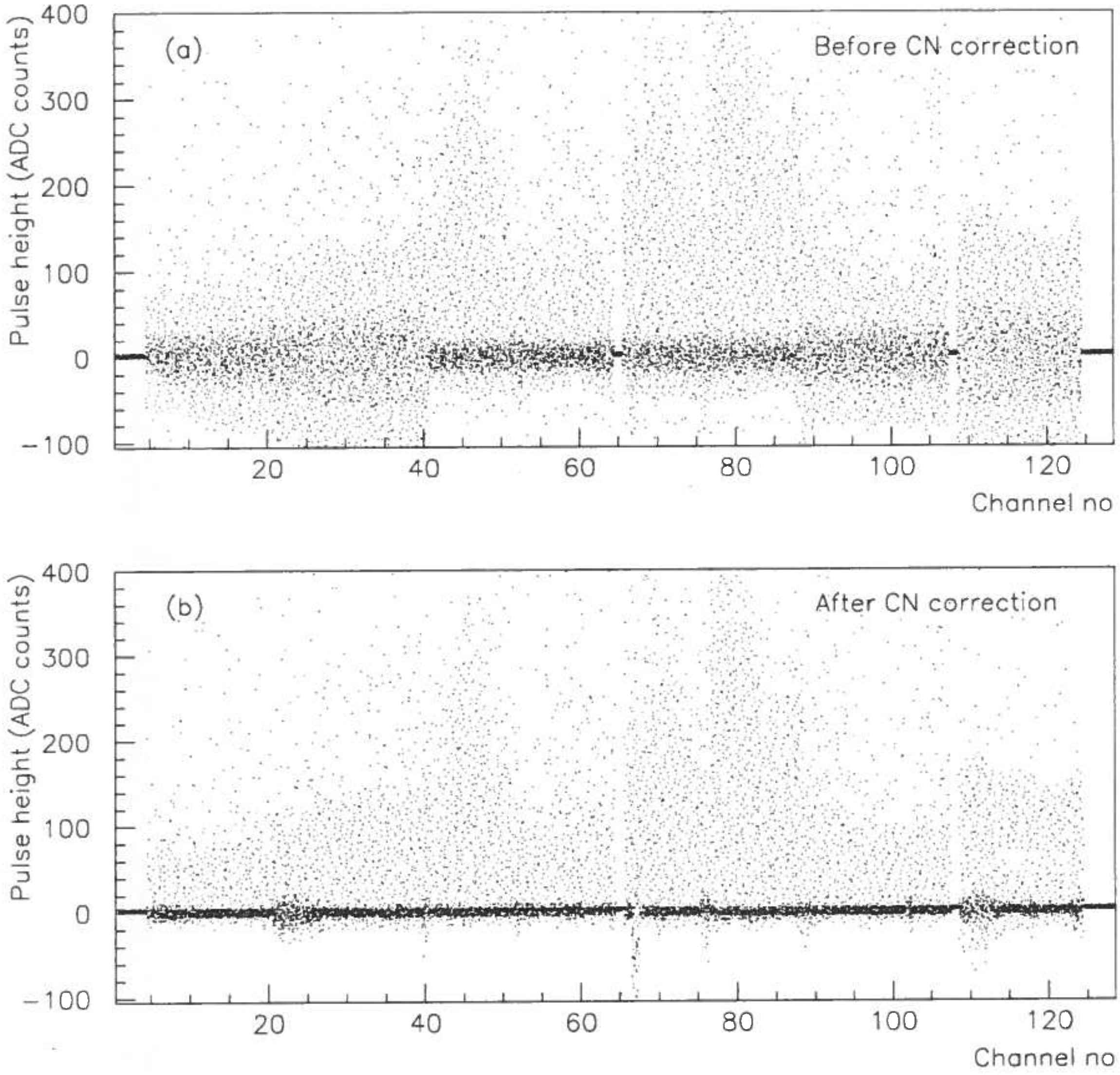

Figure 4: Pulse heights of the strips of a fan-in card reading out side A, (a) before and (b) after coherent-noise correction.

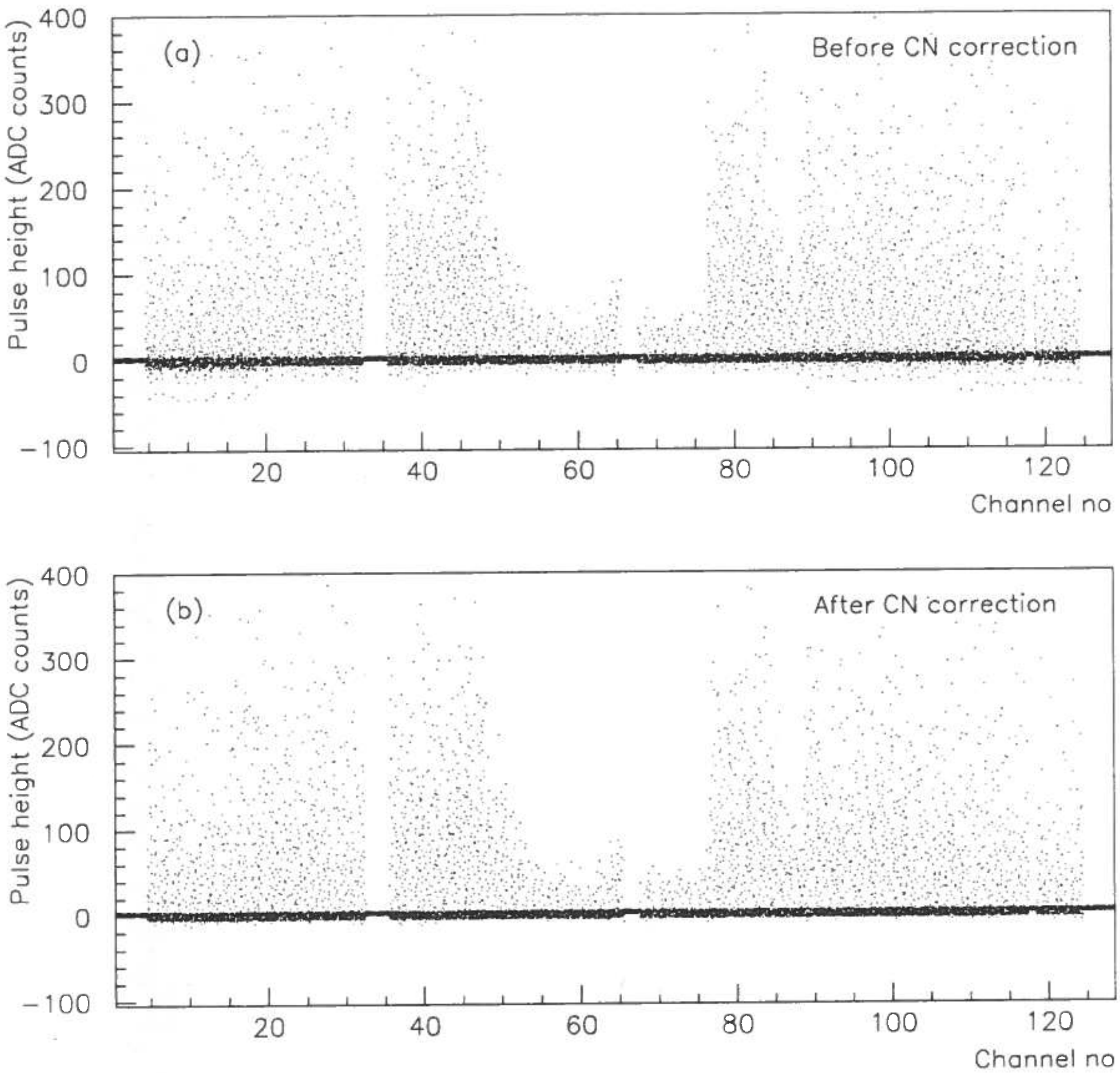

Figure 5: Pulse heights of the strips of a fan-in card reading out side C, (a) before and (b) after coherent-noise correction.

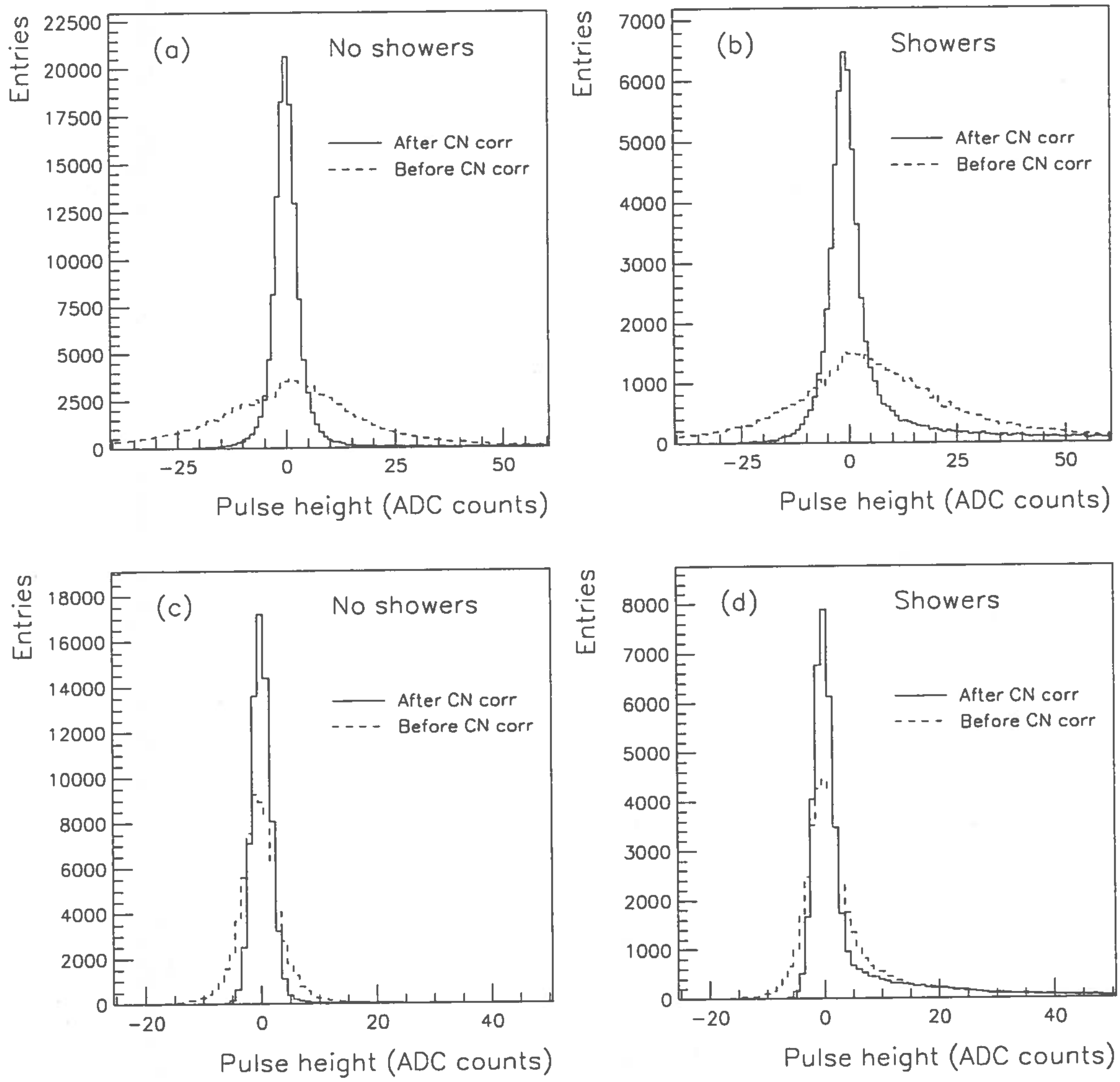

Figure 6: Pulse-height distributions of all strips of a fan-in card before and after coherent-noise correction, for a fan-in card of side A (a) without and (b) with showers and one of side C (c) without and (d) with showers.

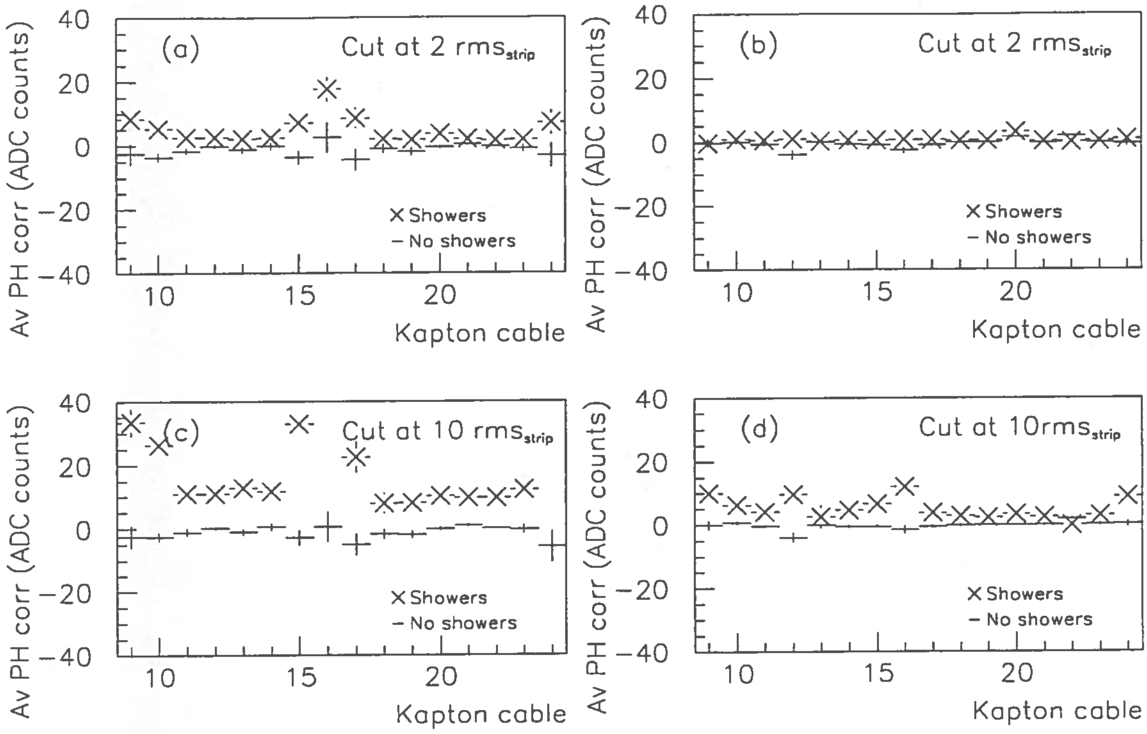

Figure 7: Average pulse-height correction in the presence and in the absence of showers for some Kapton cables. (a) and (b) show examples from side A and side C respectively, when a cut at $2r_i$ was used in the calculation of $< a >_k$. (c) and (d) show the same Kapton cables when a cut at $10r_i$ was used instead.

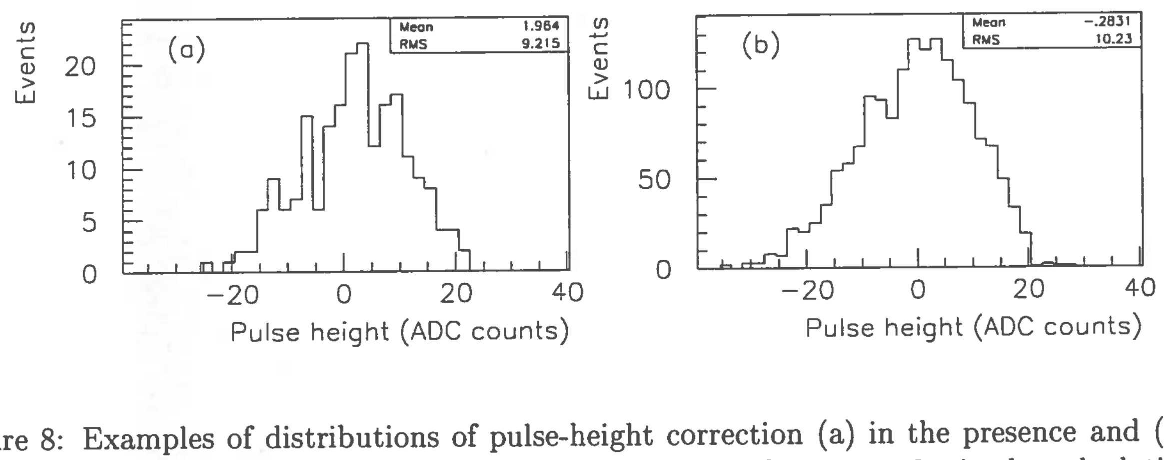

Figure 8: Examples of distributions of pulse-height correction (a) in the presence and (b) in the absence of showers for a Kapton cable of side A and with a cut at $2r_i$ in the calculation of $< a >_k$.

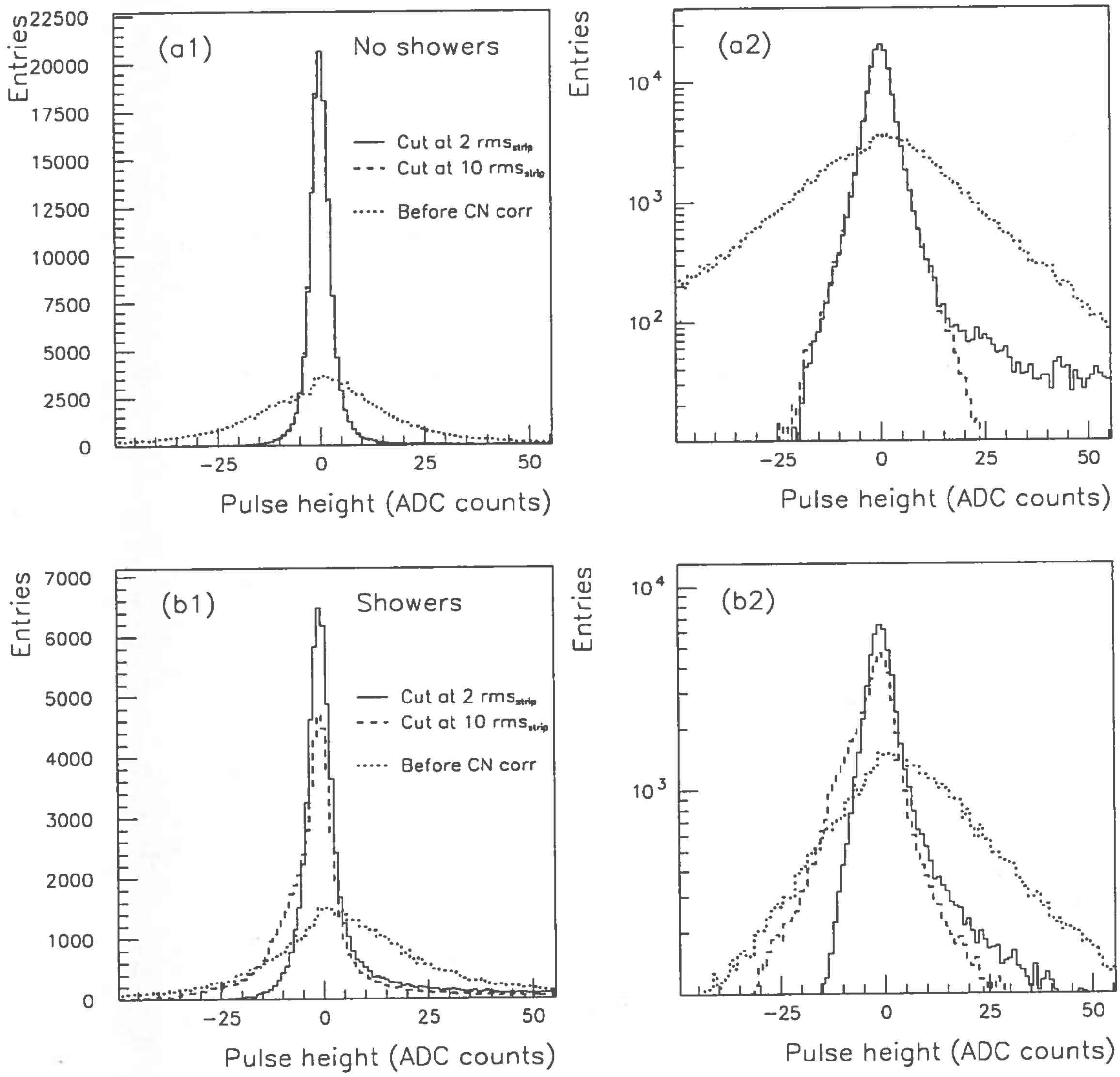

Figure 9: Pulse-height distributions of all strips of a fan-in card of side A after coherent-noise correction; cut at $10r_i$ *vs.* cut at $2r_i$ in the calculation of $< a >_k$. (a1) and (a2) show the distributions in the absence of showers, on linear and logarithmic scales respectively, whereas (b1) and (b2) show the distributions in the presence of showers, also on linear and logarithmic scales.

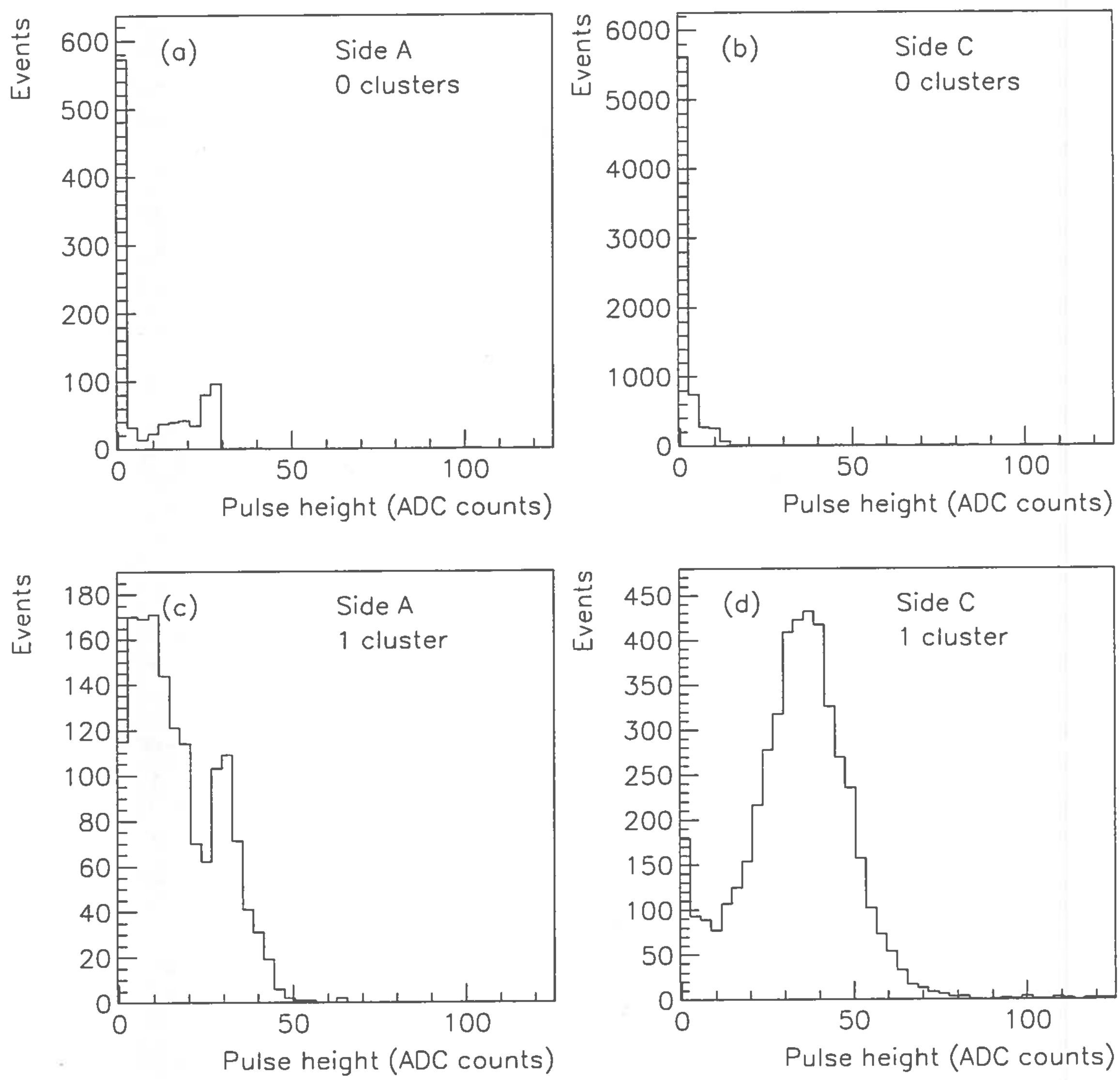

Figure 10: Example of number of strips to read out after a cut at $3r_i$ for sides A and C, with the calorimeter indicating 0 and 1 clusters (showers) respectively.

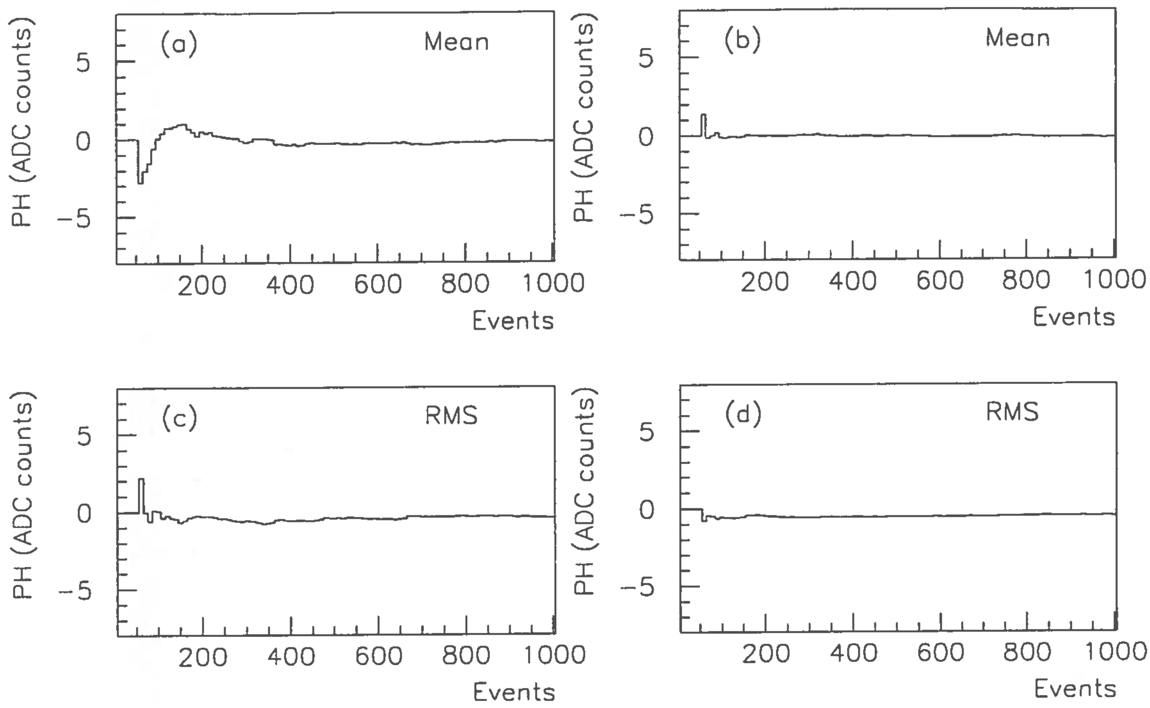

Figure 11: Examples of difference in mean and in RMS between pedestals calculated on-line and those calculated off-line as a function of the number of events. (a) and (c) show a strip from side A, and (b) and (d) show a strip from side C. The first 50 events were used to calculate preliminary pedestals according to the first step of the algorithm.

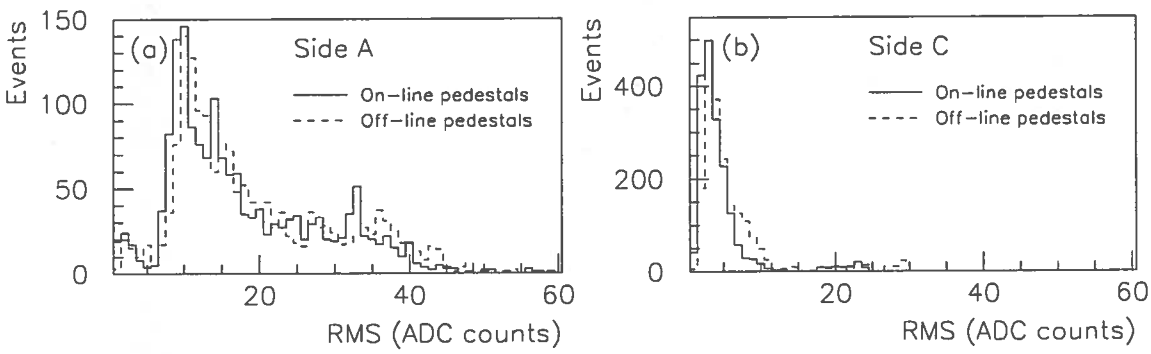

Figure 12: Comparison between RMS distributions of pedestals calculated on-line and off-line respectively for side A and side C. (Each strip provides one entry in the histograms.)

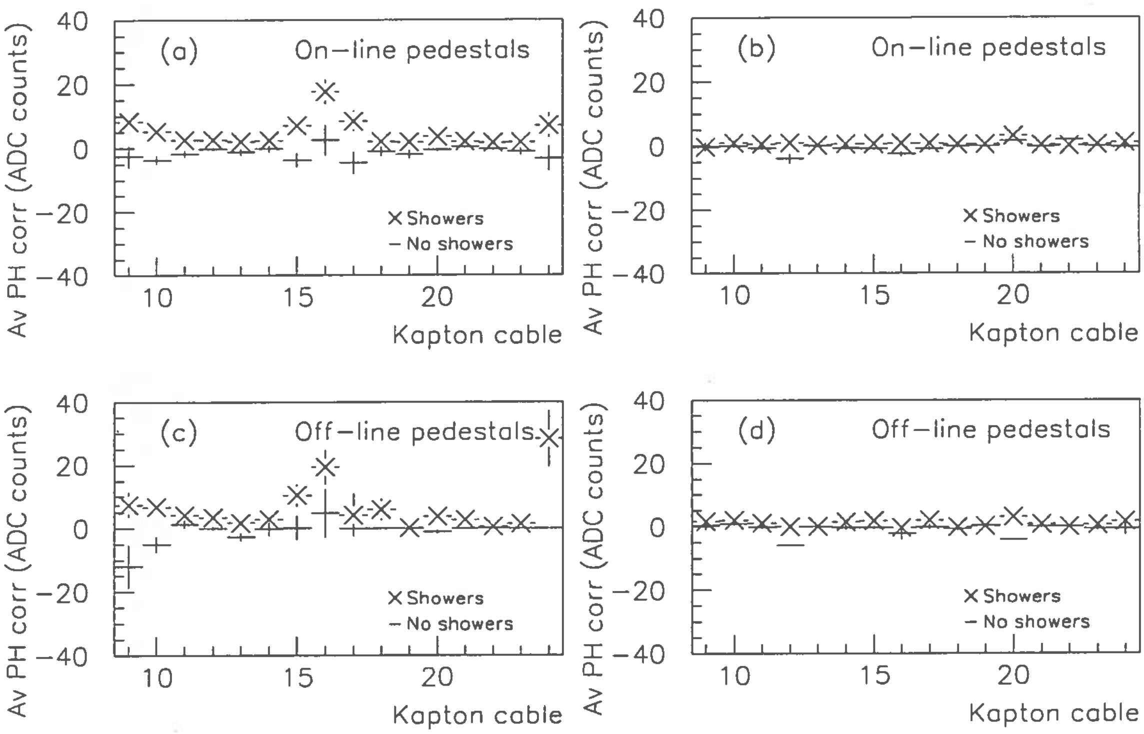

Figure 13: Example of average pulse-height correction using on-line pedestals, (a) side A and (b) side C, and off-line pedestals, (c) side A and (d) side C.

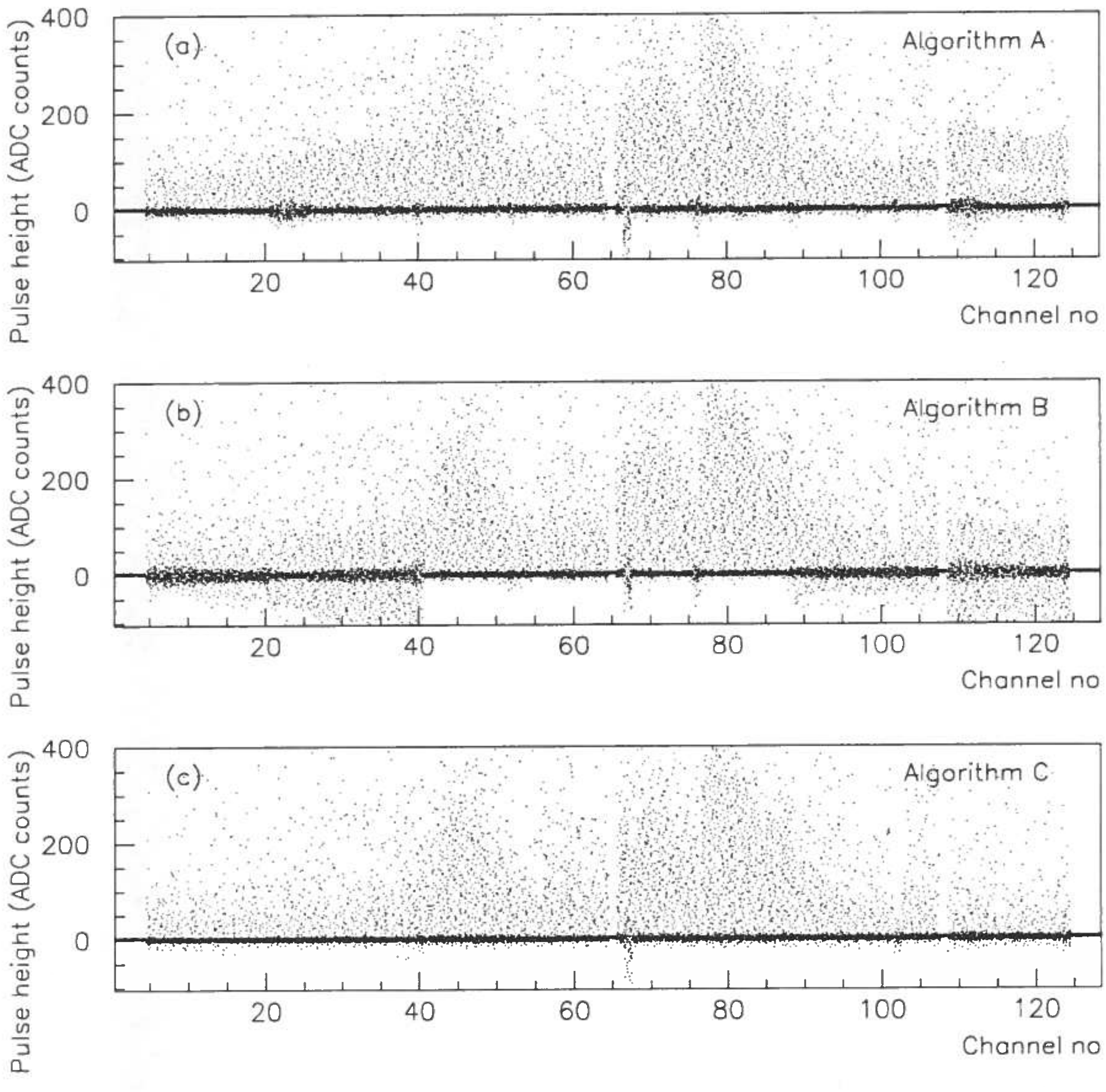

Figure 14: Pulse heights after coherent-noise correction of a fan-in card of side A for the three methods.

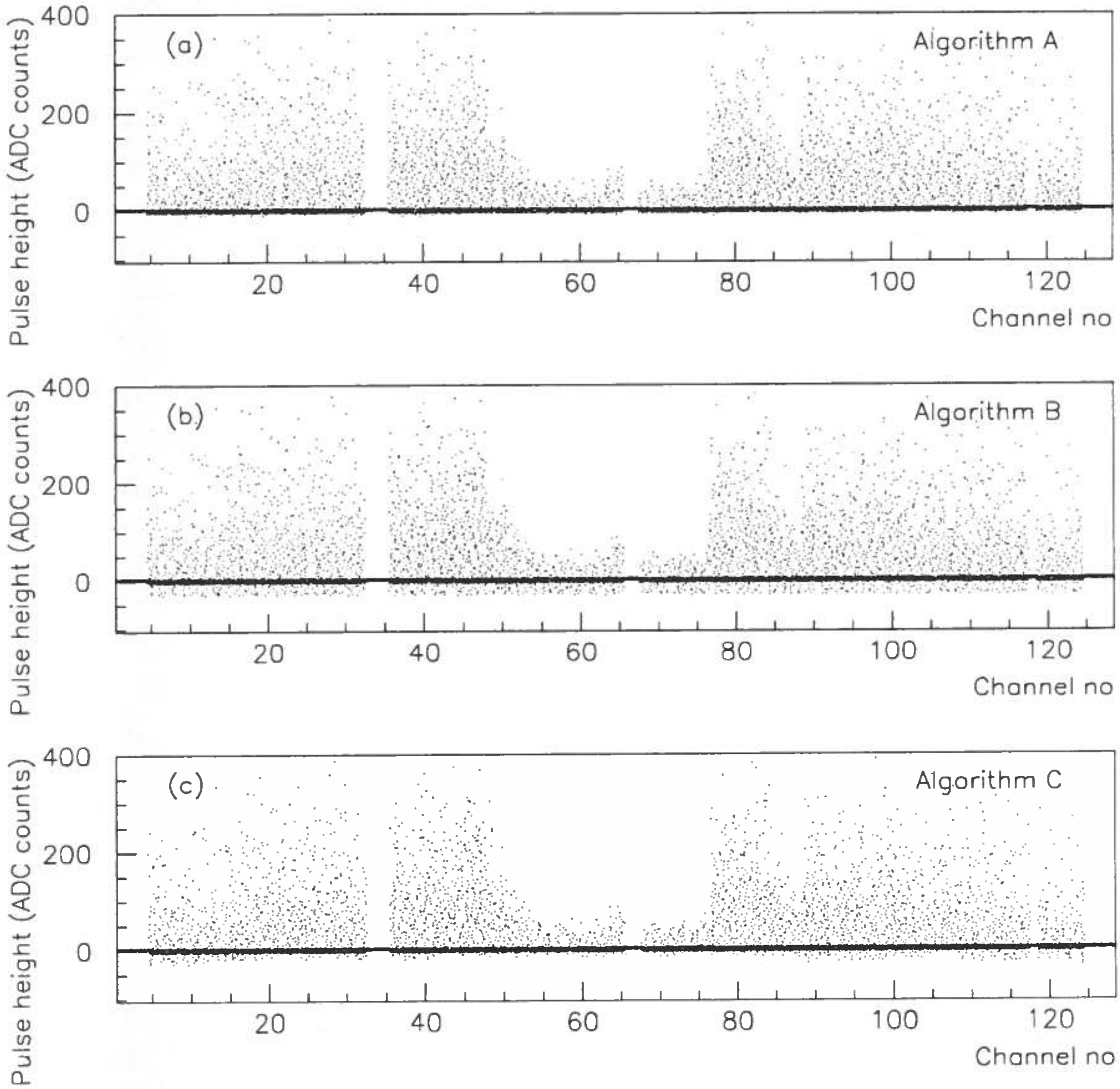

Figure 15: Pulse heights after coherent-noise correction of a fan-in card of side C for the three methods.

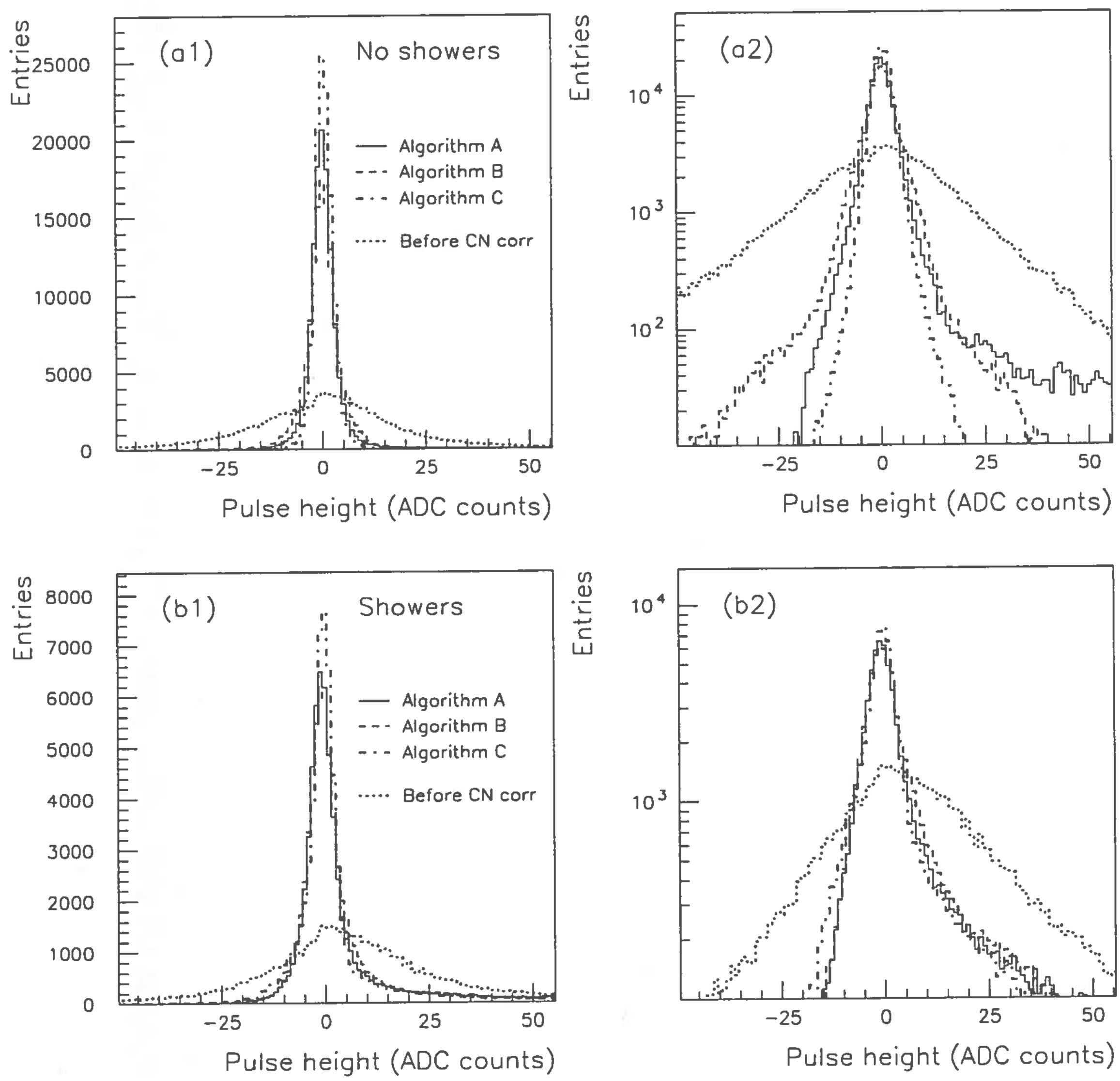

Figure 16: Pulse-height distributions after coherent-noise correction of all strips of a fan-in card of side A for each one of the three algorithms. (a1) and (a2) show the distributions in the absence of showers, on linear and logarithmic scales respectively, whereas (b1) and (b2) show the distributions in the presence of showers, again on linear and logarithmic scales.

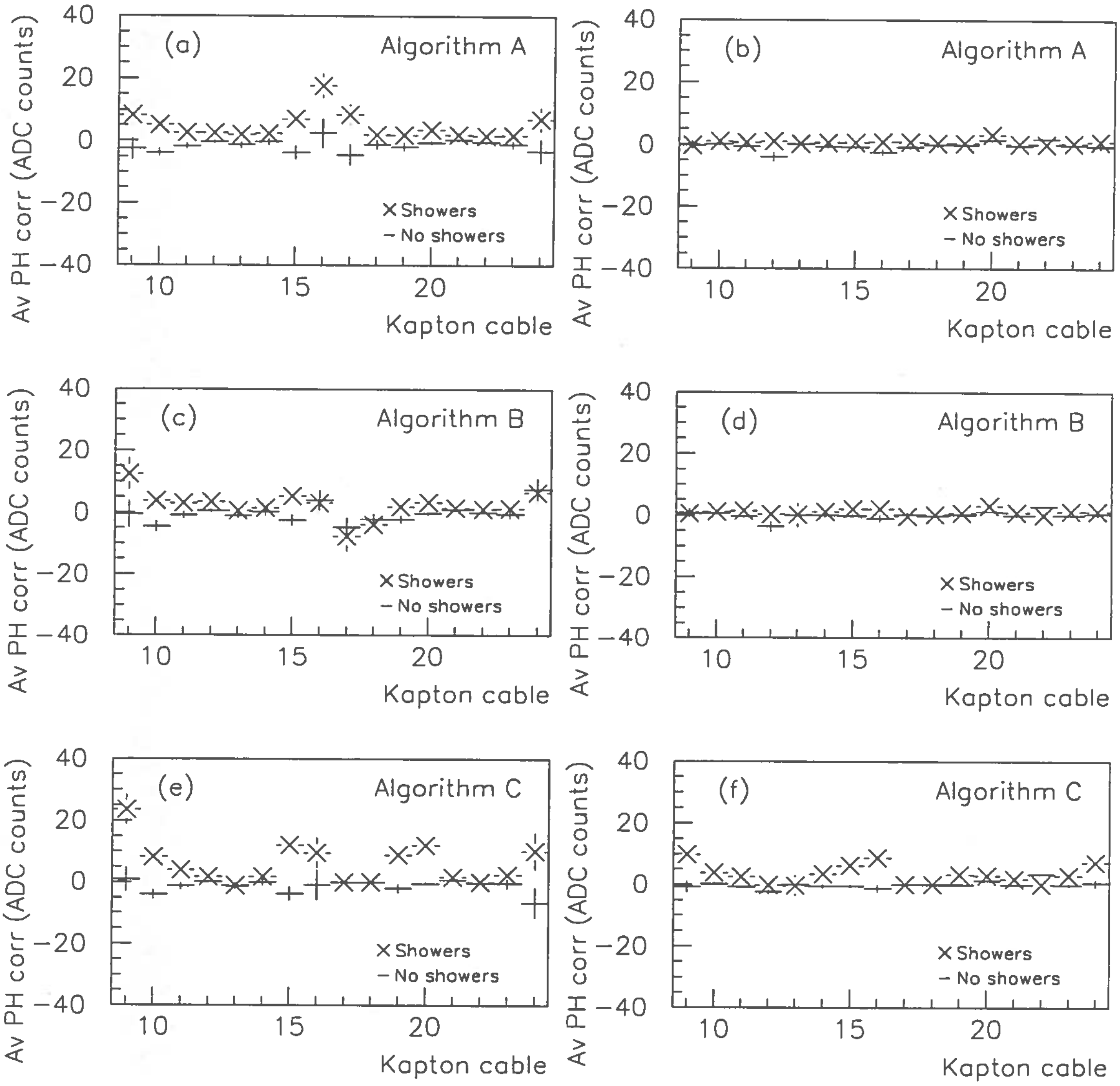

Figure 17: Example of average pulse-height correction for the three different algorithms; (a), (c) and (e) side A and (b), (d) and (f) side C.